DOI: 10.1002/ange.200803427

CO Oxidation

Generating Highly Active Partially Oxidized Platinum during Oxidation of Carbon Monoxide over Pt/Al_2O_3: In Situ, Time-Resolved, and High-Energy-Resolution X-Ray Absorption Spectroscopy**

*Jagdeep Singh, Evalyn M. C. Alayon, Moniek Tromp, Olga V. Safonova, Pieter Glatzel, Maarten Nachtegaal, Ronald Frahm, and Jeroen A. van Bokhoven**

Dedicated to the Catalysis Society of Japan on the occasion of its 50th anniversary

The oxidation of carbon monoxide is one of the most intensely studied reactions in heterogeneous catalysis. The preferential oxidation of carbon monoxide in a hydrogen-rich mixture is of considerable interest for the technical purification of the hydrogen feed gas.[1] Furthermore, because platinum is an active component of automotive three-way catalysts, the determination of the active structure of platinum for the oxidation of carbon monoxide, nitric oxide, and hydrocarbons in the exhaust is relevant.[2] Ertl and co-workers showed that on single crystals under low-pressure conditions, varying reconstruction of the platinum surface, which occurs after the adsorption of carbon monoxide, leads to domains rich in carbon monoxide and in oxygen that have different reaction rates.[3] In a low-activity regime over Pt(111), carbon monoxide is bound to the surface, and the rate-limiting step is the desorption of this carbon monoxide.[4] The activation energy of the reaction after ignition is lowered from 176 to 59 $kJ\,mol^{-1}$. Similarly, on supported metal catalysts, little or no adsorbed carbon monoxide was detected under the high-activity conditions.[5]

Most researchers claim that metallic platinum is the active surface species for oxidation of carbon monoxide even in an oxygen-rich environment.[5b,6] Recent surface X-ray diffraction studies on surfaces of platinum single crystals,[7] on the other hand, indicate that the rate of oxidation of carbon monoxide is higher when the surface is oxidized. Finally, it has been suggested that the active structure is a combination of metallic and oxidic phases on the supported metal catalysts.[8,9] Theoretical calculations have shown the important role played by partially oxidized metal surfaces in generating high catalytic activity over metal surfaces.[10] Furthermore, scanning tunnelling microscopy revealed the high reactivity of an oxygen-rich ruthenium surface in the oxidation of carbon monoxide.[11]

We have studied the structure of a working supported metal catalyst in a plug-flow reactor,[12d] combining in situ, time-resolved, and high-energy-resolution fluorescence detected X-ray absorption spectroscopy (HERFD XAS) with kinetic measurements by means of mass spectrometry, thus bridging the materials and pressure gaps. We demonstrate a highly dynamic behavior of the reactivity and structure of the catalyst under changing conditions. XAS provides the local electronic and geometric structure of the platinum species. The intensity of the whiteline of an L_3 edge XAS spectrum reveals the unfilled d band and is sensitive to the metal oxidation state and the presence of adsorbates on the surface.[12d,13] The use of HERFD XAS improves the resolution of the spectra.[12b–e] The sharper features in these spectra originate from the decreased final state core–hole lifetime broadening of one particular fluorescence channel, as detected by a secondary energy-selective spectrometer.[12a,c,e] Therefore, HERFD XAS provides more insight into the geometric and electronic structures of the active metal. We have established the influence of temperature and the ratio between carbon monoxide and oxygen on the rate of oxidation of carbon monoxide and on the structure of platinum under those conditions.

Figure 1 shows the rate of oxidation of carbon monoxide as a function of temperature (5 $K\,min^{-1}$) at various oxygen/carbon monoxide ratios. At any particular temperature, higher oxygen concentrations always showed higher conversion, indicating a positive effect of the oxygen pressure on the conversion of carbon monoxide.[4,14] While increasing the temperature, at a particular temperature there was a sudden increase in activity to the high-activity regime. This so-called ignition occurred at lower temperature with increasing oxygen concentration (Table 1), which is in agreement with previous findings.[3b,4,5b,14d,a] Heating was continued until the

---

[*] J. Singh, E. M. C. Alayon, Prof. Dr. J. A. van Bokhoven
Institute of Chemical and Bioengineering, ETH Zürich
8093 Zürich (Switzerland)
Fax: (+41) 43-362-1162
E-mail: j.a.vanbokhoven@chem.ethz.ch
Homepage: http://www.vanbokhoven.ethz.ch/
Dr. M. Tromp
School of Chemistry, University of Southampton (UK)
Dr. O. V. Safonova
Swiss Norwegian Beamlines (SNBL), ESRF, Grenoble (France)
Dr. P. Glatzel
European Synchrotron Radiation Facility (ESRF), Grenoble (France)
Dr. M. Nachtegaal
Paul Scherrer Institut, Villigen (Switzerland)
Prof. Dr. R. Frahm
Fachbereich C/Physik, Universität Wuppertal (Germany)

[**] This work was supported by the EPSRC (EP/E060404/1) (M.T.) and the Swiss National Science Foundation (SNF) (J.S., E.M.C.A., J.A.v.B.) E.M.C.A. thanks the MAMASELF programme for financial support.

Supporting information for this article is available on the WWW under http://dx.doi.org/10.1002/anie.200803427.

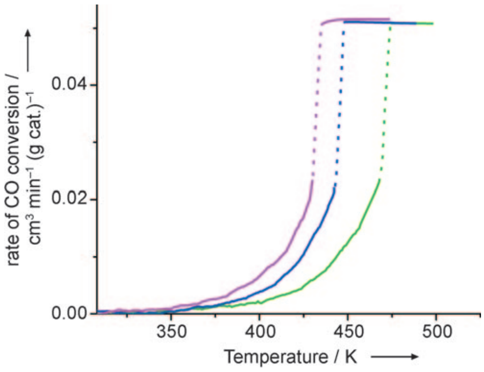

Figure 1. Rate of oxidation of carbon monoxide over 2 wt% Pt/Al_2O_3 a) during heating (5 K min^{-1}) at oxygen/carbon monoxide ratios of 1:1 (green), 2:1 (blue), and 5:1 (pink).

Table 1: Results of kinetic measurements of oxidation of carbon monoxide over a 2 wt% Pt/Al_2O_3 catalyst.

O_2/CO	Ignition or extinction temperature [K] heating	cooling	Hysteresis	Temperature at onset of conversion [K]
1:1	472	456	yes	340
2:1	445	440	yes	338
5:1	433	421	yes	329

rate of oxidation of carbon monoxide was constant and the conversion of carbon monoxide was complete. As the temperature decreased, the rate of oxidation of carbon monoxide also decreased until, at a specific temperature, the reaction rate decreased suddenly, which is the so-called extinction. At all oxygen/carbon monoxide ratios, hysteresis occurred between ignition and extinction temperatures (Table 1). Table 1 also shows the temperature at the onset of carbon monoxide conversion.

Figure 2 shows the in situ Pt L_3 edge HERFD XAS spectra of Pt/Al_2O_3 as a function of temperature and thus conversion at oxygen/carbon monoxide ratios of 1:1. Spectra were obtained every two minutes. Large changes occurred between spectra taken below and above the ignition temperature. Below ignition, a whiteline (i.e. the first feature in the L_3 edge spectrum) of low intensity was observed at 11569 eV. Moreover, it displayed a double feature, which is characteristic of adsorbed carbon monoxide on the platinum particles.[12d] With increasing temperature, the intensity of the shoulder decreased, which indicates desorption of carbon monoxide. Under a stream of oxygen/carbon monoxide (1:1) at 475 K (Figure 2a), at a temperature above the ignition temperature, the spectra showed a strong increase in the intensity of the whiteline while the edge energy shifted to lower energy, which is characteristic of oxidized platinum.[12d] At this point, the conversion of carbon monoxide was almost complete (Figure 1). The XAS spectra showed no further changes at higher temperatures. The spectra above ignition show very little structure above the whiteline, which suggests an amorphous structure of the oxide. Under streams of oxygen/carbon monoxide at ratios of 2:1 and 5:1, ignition occurred at lower temperatures with increasing oxygen concentration, but identical spectral changes were observed below and above ignition (Supporting Information, Figures S1a and S2a). Figure 2b shows the spectra as the catalyst cooled to 313 K under a stream of oxygen/carbon monoxide (1:1). At the extinction temperature, the intensity of the whiteline decreased and the doublet corresponding to adsorbed carbon monoxide reappeared. As expected, its intensity increased further with decreasing temperature, because of the re-adsorption of carbon monoxide. Again, identical behavior was observed for oxygen/carbon monoxide ratios of 2:1 and 5:1, which showed different extinction temperatures, but identical changes occurred in the spectra above and below the extinction temperature (Supporting Information, Figure S1b and S2b).

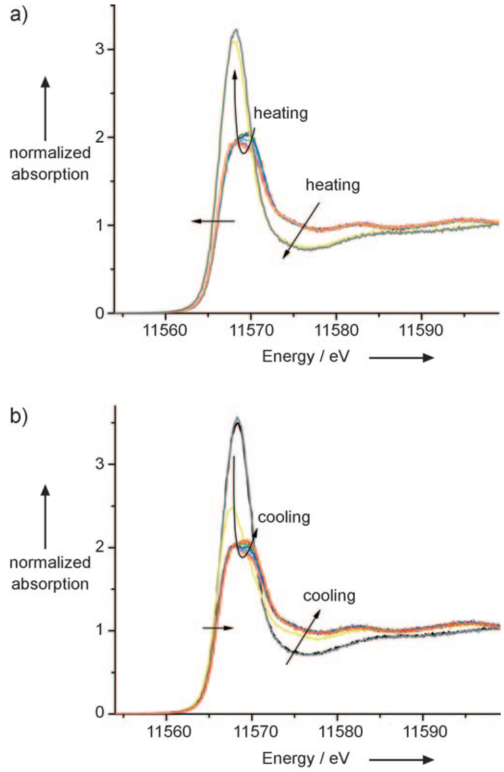

Figure 2. Pt L_3 edge HERFD XANES of 2 wt% Pt/Al_2O_3 during oxidation of carbon monoxide at an oxygen/carbon monoxide ratio of 1:1 a) measured during heating at 308 K (red), 328 K (green), 361 K (blue) 394 K (cyan), 425 K (pink), 443 K (orange), 475 K (yellow), and 491 K (gray) and b) during cooling at 503 K (black), 487 K (gray), 471 K (yellow), 453 K (orange), 421 K (pink), 387 K (cyan), 359 K (blue), 331 K (green), and 313 K (red). The ignition and extinction temperatures were 472 and 456 K, respectively. The arrows indicate the trends.

To determine the structure of the platinum catalyst in various gas environments, the catalyst was exposed to streams of oxygen and carbon monoxide in different ratios, either starting from pure oxygen and increasing the carbon monoxide concentration or starting from pure carbon monoxide and increasing the oxygen content. This experiment was performed below the ignition temperature. Figure S3 (Supporting Information) shows the Pt L_3 edge HERFD XAS spectra of Pt/Al_2O_3 at 398 K under these conditions. All spectra show the characteristic doublet in the whiteline, which identifies carbon monoxide adsorbed on the surface, except the spectrum that was measured under a stream of pure oxygen, which showed the high-intensity whiteline of oxidized platinum. The spectra indicate that traces of carbon monoxide are sufficient to reduce a pre-oxidized catalyst.

The two reaction regimes[3b,4,5,14d] are characterized by different structures of the platinum particles. At low activity, adsorbed carbon monoxide on reduced platinum was observed (Figure 2), in general agreement with IR spectroscopy data,[5b,6a,14b,d] and at high activity, a large fraction of oxidized platinum was observed. High activity is found only at elevated temperature (Figure 1).[6a] On the basis of our in situ HERFD XAS data, the high-activity regime is characterized by the presence of large amounts of oxidic platinum. Earlier IR spectroscopy studies showed that there is a minimal amount or no carbon monoxide on the surface of the catalyst at high temperature,[4,5b,d,12b,17] which agrees with the surface of the catalyst being largely oxidic. There is a very sudden change in catalyst performance, which is paralleled by structural changes.

Insights into the structural changes that occurred during ignition were obtained with quick extended X-ray absorption fine structure (QEXAFS).[15,16] Figure 3 shows the spectra that were recorded with a time resolution of 0.5 s. For clarity, not all recorded spectra are shown. As soon as the ignition started, the whiteline increased in intensity. After only 9 s the changes in the spectra were complete. In this time period, the conversion of carbon monoxide increased from 53 to 89% (Figure 3b). The isobestic points in Figure 3a indicate that there is a direct conversion of reduced platinum to partially oxidized platinum.

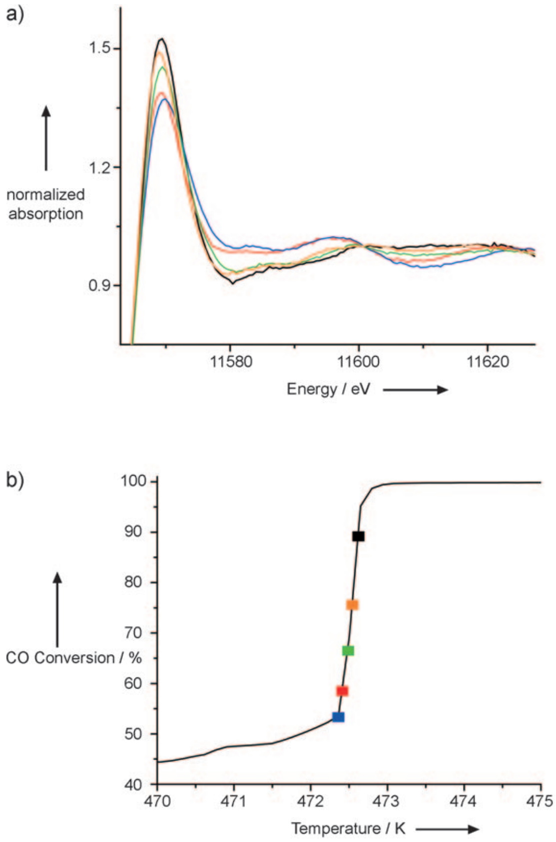

Figure 3. Pt L_3 edge XANES of 2 wt% Pt/Al_2O_3 recorded in QEXAFS mode a) taken at start of ignition (blue) and 1.5 (red), 4 (green), 6.5 (orange), and 9 s (black) after start of ignition during heating at a rate of 2 $K\,min^{-1}$; b) percentage conversion of carbon monoxide during ignition, color coding of the squares correlates to the spectra in (a).

The in situ HERFD XAS and QEXAFS data suggest that oxidized platinum plays an active role in generating high activity. As soon as the surface is sufficiently depleted of carbon monoxide, oxygen reacts with the platinum surface, with a simultaneous increase of rate of oxidation of carbon monoxide. This decreases the concentration of carbon monoxide in the gas phase and further depletes the surface of carbon monoxide and subsequently increases the extent of surface oxidation, which additionally enhances the rate of reaction. The result is the autocatalytic enhancement in conversion.

Figure 4 shows a diagram that gives an overview of the oxidation of carbon monoxide over supported platinum nanoparticles. Below the ignition temperature, the surface is covered with carbon monoxide, and the reaction rate is low and determined by the desorption of carbon monoxide. At these temperatures, the platinum particles are reduced with adsorbed carbon monoxide, even in an oxygen-rich environment. As the temperature increases, some of the carbon monoxide is converted and increasingly desorbs from the platinum surface. At the ignition temperature, oxidic platinum forms and the rate suddenly increases. At high activity and temperatures above the ignition temperature, the particles are largely oxidic, which is proposed to be required to generate the highly active state of the catalyst.

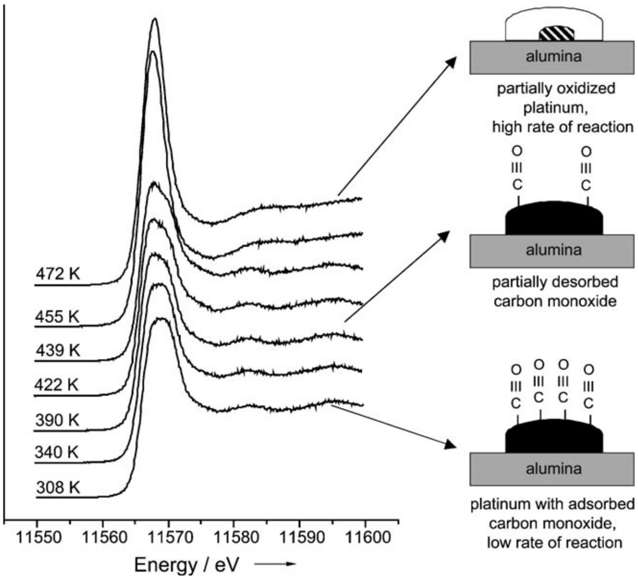

Figure 4. Diagram of oxidation of carbon monoxide over 2 wt% Pt/Al_2O_3.

The oxidation of carbon monoxide over alumina-supported platinum nanoparticles is sensitive to both the gas composition and the temperature. In situ HERFD XAS spectroscopy distinguished the active phases in the low- and the high-activity regimes: platinum with adsorbed carbon monoxide in the low-activity regime and oxidic platinum in the high-activity regime. Kinetics studies by mass spectroscopy identified the rapid change in the activity, which is paralleled by rapid change in catalyst structure, as identified by QEXAFS. The ignition and extinction occur suddenly, because the formation and disappearance of the more active phase are autocatalytic. High temperature and a high oxygen concentration are required to obtain the more active oxidic platinum catalyst.

Experimental Section

The catalyst was prepared by incipient-wetness impregnation. Tetraammine platinum nitrate (0.197 g) was dissolved in water (2.55 mL) and then impregnated on alumina (5 g), which was dried at 393 K, to give 2 wt % Pt/Al_2O_3 samples. The resulting powder was dried at room temperature for four hours. Calcination was performed in flowing air in two steps: heating to 473 K and maintaining that temperature for four hours, and then heating to 673 K and maintaining that temperature for four hours. The heating rate during both temperature increases was 5 $K\,min^{-1}$. The catalyst was subsequently reduced in a flow of pure hydrogen at 723 K for two hours to yield 2 wt % platinum nanoparticles supported on alumina. The particle size was determined by scanning transmission electron microscopy (Supporting Information, Figure S4). The sample was immersed in ethanol and placed on carbon foil supported on a copper grid after the evaporation of the ethanol. The measurements were performed using a Tecnai F30 microscope operating with a field-emission cathode at 300 kV using a high-angle annular dark-field (HAADF) detector. Energy-dispersive X-ray spectroscopy (EDX) with a detector attached to a Tecnai F30 microscope revealed that the miniscule bright spots were platinum nanoparticles. Figure S4 (Supporting Information) shows a dark-field micrograph of the catalyst and a particle-size distribution around 0.9 nm.

All gases were ultrapure and mixed to give the desired ratio of oxygen and carbon monoxide by means of six mass-flow controllers (MFCs), all of which were computer-controlled. The exhaust of the reactor was connected to a QIC-20 mass spectrometer (Hiden Analytical) to monitor the outlet gases. The reactor was equipped with a transmission/fluorescence cell with aluminium windows to allow XAS experimentation. The reactor was based on a model[17] that resembles a plug-flow reactor with a diameter of 1.6 mm. The temperature of the catalyst system was monitored by a thermocouple in the reactor holder. The catalyst was sieved to a fraction of 255–325 μm particles. The amount of catalyst in the reactor was approximately 18 mg. The catalyst was treated in situ in 2 % hydrogen in helium at 473 K before each experiment. Subsequently, the catalyst was exposed to an atmosphere of carbon monoxide and oxygen in varying mixtures. The partial pressure of carbon monoxide in all the experiments was kept constant at 0.04 bar. The conversion of carbon monoxide was monitored using the mass spectrometer and used to calculate the rate of reaction. The measurements were done at a constant total flux of 25 $mL\,min^{-1}$ through the reactor, corresponding to a space velocity of about 54 000 h^{-1}.

High-energy-resolution X-ray absorption experiments were carried out at beamline ID 26 at the European Synchrotron Radiation Facility (ESRF), Grenoble, France. The electron energy was 6.0 GeV, and the ring current varied from 50 to 90 mA. Two u35 undulators were used to perform the measurements. The X-ray beam measured 0.3 mm across and 1 mm high; the total flux was 5×10^{12} $photons\,s^{-1}$. The energy scale was calibrated with a Pt foil. The incident energy was selected by means of a pair of Si(111) crystals with an energy bandwidth of 1.5 eV at the Pt L_3 edge. Higher harmonics were suppressed using two mirrors, one coated with Pd and the other with Cr, working at 3 mrad in total reflection. High-energy-resolution emission detection was carried out with a horizontal-plane Rowland circle spectrometer that was tuned to the Pt $L\alpha_1$ (9442 eV) fluorescence line. A total energy bandwidth (incident energy convoluted with emission detection) of 1.8 eV was achieved with the (660) Bragg reflection of one spherically bent Ge wafer (R = 1000 mm). This is below the HERFD lifetime broadening of 2.2 eV when based on the Pt $L_{\alpha1}$ line. The $2p_{3/2}$ core hole lifetime broadening is 5.2 eV. The detector was an avalanche photodiode (APD). A Canberra silicon photodiode was mounted to measure the total fluorescence simultaneously with the HERFD XAS. Spectra were collected before and during heating of the sample at 5 $K\,min^{-1}$ to the temperature of maximum conversion; the ratio of oxygen to carbon monoxide was increased from 1:1 to 5:1 in an oxygen-rich environment. Furthermore, at constant temperature, spectra were collected at various ratios of oxygen to carbon monoxide, starting with a pre-oxidized sample and then decreasing the ratio as well as starting with a catalyst pre-reduced in carbon monoxide and then increasing the ratio. Each HERFD XANES scan took one minute, after which a one-minute EXAFS scan was recorded to allow normalization of the data. QEXAFS experiments were carried out at the new superXAS beamline located at Swiss Light Source (SLS), Villigen, Switzerland. The ring current was approximately 400 mA and operated in top-up mode. The polychromatic radiation from a superbend magnet, with a magnetic field of 2.9 T and critical energy of 11.9 keV, was monochromatized using a channel cut Si(111) crystal in the QEXAFS monochromator.[15] The X-ray beam measured 0.1 mm across and 0.1 mm high at the sample position; the total flux was 3×10^{12} $photons\,s^{-1}$. The energy scale was calibrated with a platinum foil. Spectra were collected in transmission mode using two ionization chambers filled with air. For absolute energy calibration, the absorption of a platinum foil was always measured simultaneously between the second ionization chamber and a photodiode. The QEXAFS monochromator was oscillating at 1 Hz for the QEXAFS mode data collection, resulting in two spectra per second. Thus, QEXAFS spectra were collected with a time resolution of 0.5 seconds, during ignition and extinction while heating and cooling the sample at 2 $K\,min^{-1}$ using an oxygen/carbon monoxide ratio of 1:1.

Received: July 15, 2008

Keywords: CO oxidation · heterogeneous catalysis · platinum · X-ray absorption spectroscopy

[1] C. D. Dudfield, R. Chen, P. L. Adcock, *Int. J. Hydrogen Energy* **2001**, *26*, 763 – 775.

[2] R. J. Farrauto, R. M. Heck, *Catal. Today* **1999**, *51*, 351 – 360.

[3] a) G. Ertl, P. R. Norton, J. Ruestig, *Phys. Rev. Lett.* **1982**, *49*, 177; b) G. Ertl, *Surf. Sci.* **1993**, *287–288*, 1 – 11; c) G. Ertl, *Adv. Catal.* **1990**, *37*, 213 – 277.

[4] X. Su, P. S. Cremer, Y. R. Shen, G. A. Somorjai, *J. Am. Chem. Soc.* **1997**, *119*, 3994 – 4000.

[5] a) F. J. Gracia, L. Bollmann, E. E. Wolf, J. T. Miller, A. J. Kropf, *J. Catal.* **2003**, *220*, 382 – 391; b) P.-A. Carlsson, L. Oesterlund, P. Thormählen, A. Palmqvist, E. Fridell, J. Jansson, M. Skoglundh, *J. Catal.* **2004**, *226*, 422 – 434; c) F. J. Gracia, S. Guerrero, E. E. Wolf, J. T. Miller, A. J. Kropf, *J. Catal.* **2005**, *233*, 372 – 387; d) P.-A. Carlsson, V. P. Zhdanov, M. Skoglundh, *Phys. Chem. Chem. Phys.* **2006**, *8*, 2703 – 2706.

[6] a) T. H. Lindstrom, T. T. Tsotsis, *Surf. Sci.* **1985**, *150*, 487 – 502; b) J. A. Anderson, *J. Chem. Soc. Faraday Trans.* **1992**, *88*, 1197 – 1201; c) T. Visser, T. A. Nijhuis, A. M. J. van der Eerden, K. Jenken, Y. Ji, W. Bras, S. Nikitenko, Y. Ikeda, M. Lepage, B. M. Weckhuysen, *J. Phys. Chem. B* **2005**, *109*, 3822 – 3831.

[7] M. D. Ackermann, et al., *Phys. Rev. Lett.* **2005**, *95*, 255505 (see the Supporting Information).

[8] R. Burch, P. K. Loader, *Appl. Catal. B* **1994**, *5*, 149 – 164.

[9] S. Yang, A. Maroto-Valiente, M. Benito-Gonzalez, I. Rodriguez-Ramos, A. Guerrero-Ruiz, *Appl. Catal. B* **2000**, *28*, 223 – 233.

[10] a) C. Stampfl, M. Scheffler, *Phys. Rev. Lett.* **1997**, *78*, 1500; b) X.-G. Wang, A. Chaka, M. Scheffler, *Phys. Rev. Lett.* **2000**, *84*, 3650; c) K. Reuter, M. Scheffler, *Phys. Rev. B* **2001**, *65*, 035406; d) K. Reuter, M. Scheffler, *Phys. Rev. B* **2003**, *68*, 045407.

[11] H. Over, Y. D. Kim, A. P. Seitsonen, S. Wendt, E. Lundgren, M. Schmid, P. Varga, A. Morgante, G. Ertl, *Science* **2000**, *287*, 1474 – 1476.

[12] a) K. Hämäläinen, D. P. Siddons, J. B. Hastings, L. E. Berman, *Phys. Rev. Lett.* **1991**, *67*, 2850 – 2853; b) F. M. F. de Groot, *Coord. Chem. Rev.* **2005**, *249*, 31 – 63; c) P. Glatzel, U. Bergmann, *Coord. Chem. Rev.* **2005**, *249*, 65 – 95; d) O. V. Safonova, M. Tromp, J. A. van Bokhoven, F. M. F. de Groot, J. Evans, P. Glatzel, *J. Phys. Chem. B* **2006**, *110*, 16162 – 16164; e) J. A. van Bokhoven, C. Louis. J. T. Miller, M. Tromp, O. V. Safonova, P. Glatzel, *Angew. Chem.* **2006**, *118*, 4767 – 4770; *Angew. Chem. Int. Ed.* **2006**, *45*, 4651 – 4654.

[13] a) D. E. Ramaker, D. C. Koningsberger, *Phys. Rev. Lett.* **2002**, *89*, 139701; b) A. L. Ankudinov, J. J. Rehr, J. J. Low, S. R. Bare, *Phys. Rev. Lett.* **2002**, *89*, 139702; c) M. K. Oudenhuijzen, J. A. van Bokhoven, J. T. Miller, D. E. Ramaker, D. C. Koningsberger, *J. Am. Chem. Soc.* **2005**, *127*, 1530 – 1540.

[14] a) N. W. Cant, P. C. Hicks, B. S. Lennon, *J. Catal.* **1978**, *54*, 372 – 383; b) D. M. Haaland, F. L. Williams, *J. Catal.* **1982**, *76*, 450 – 465; c) Y.-E. Li, D. Boeker, R. D. Gonzalez, *J. Catal.* **1988**, *110*, 319 – 329; d) P. T. Fanson, W. N. Delgass, J. Lauterbach, *J. Catal.* **2001**, *204*, 35 – 52.

[15] a) R. Frahm, *Nucl. Instrum. Methods Phys. Res. Sect. A* **1988**, *270*, 578 – 581; b) R. Frahm, *Rev. Sci. Instrum.* **1989**, *60*, 2515 – 2518; c) R. Frahm, B. Griesebock, M. Richwin, D. Lützenkirchen-Hecht, *Proc. 8th Int. Conf. Synchrotron Radiation Instumentation* (San Francisco, USA) **2004**, pp. 1411–1414; d) R. Frahm, B. Griesebock, D. Luetzenkirchen-Hecht, *Phys. Scr.* **2005**, *T115*, 974 – 976.

[16] A. J. Dent, *Top. Catal.* **2002**, *18*, 27 – 35.

[17] N. Weiher, E. Bus, B. Gorzolnik, M. Moeller, R. Prins, J. A. van Bokhoven, *J. Synchrotron Radiat.* **2005**, *12*, 675 – 679.